Large Amplitude Free Vibration of thick Laminated Composite Plates with Magnetorheological Core Via a New Sinusoidal Shear Deformation Theory

Mehdi Keshavarzian[*1], Ehsan Afshari[2]

[1] Mehdi Keshavarzian, PhD , *Email:* m-keshavarzian@malayeriau.ac.ir *ORCID:* 0000-0003-3660-4693

Department of Mechanical Engineering, Technical and Vocational University (TVU), Tehran, Iran

[*2] Ehsan Afshari,Ms.C, *Email*: ehsan.a235@gmail.com *ORCID:* 0009-0002-5306-6217

Department of Mechanical Engineering, Technical and Vocational University (TVU), Tehran, Iran.

[*]*Corresponding Author:* Mehdi Keshavarzian , *Email:* m-keshavarzian@malayeriau.ac.ir *ORCID:* 0000-0003-3660-4693

ABSTRACT

Large amplitude free vibrations have nonlinear behavior that may be detrimental to structures .As a result, they need to be effectively regulated .A composite sandwich panel with a magnetorheological (MR) core's nonlinear vibration was examined, and the softening and hardening behaviors were investigated utilizing the New Sinusoidal Shear Deformation Theory. The extraction of the governing equations and boundary conditions was made possible by Hamilton's principle. Using the harmonic balancing approach, the equation was solved analytically with cubic and quadratic nonlinearities, followed by comparing the data with the proven findings. The utilization of Galerkin's approximation approach led to the development of ordinary differential equations from the governing PDEs.When aspect ratio, damping parameter and sandwich panel thickness values increase, the vibration amplitude reduces. It is used to describe a rise in amplitude that causes a rise in nonlinear frequency. The structure's inherent frequency increased as the MR layer's thickness increased. Sandwich panels that are thick and orthotropic were found to exhibit a more significant hardening behavior.As the magnetic field grows, the structure substantially hardens in the nonlinear state, improving the stability of the system. For controlling the vibration behavior, raising the magnetic field declines the structure frequency and elevates the aspect ratio of panel raises the frequency.

Keywords: Harmonic balance; Magnetorheological core; Large amplitude; Nonlinear vibration

1. INTRODUCTION

Durable and lightweight composites have found effective applications across various fields in material science and engineering. Since laminated composite plates can be used in hostile situations, their nonlinear vibration has drawn a lot of attention. Accurately identifying

the nonlinear vibration's frequency is crucial for fitting a range of material applications. Chandra explored the significant deflection vibration of cross-ply laminated plates under specific edge conditions[1] . Chandra et al. delved into the analysis of significant deflection vibration of angle-ply laminated plates [2]. The nonlinear vibrations of simply supported rectangular cross-ply plates were investigated by Singh and co-researchers[3]. Singh and colleagues presented the extensive amplitude free vibration of simply supported antisymmetric cross-ply plates [4]. Amabili and collaborators examined the nonlinear vibrations of rectangular laminated composite plates under various boundary conditions [5]. Particularly, they compared numerical outcomes from the classical Von Karman theory, the FSDT, and the third-order shear deformation theory (TSDT). Khorshidi investigated the nonlinear elasto-plastic impact response of a moderately thick rectangular plate[6] . Yazdi conducted an analysis of the nonlinear vibration behavior of functionally graded plates using the Homotopy Perturbation Method (HPM) [7] . Quan and colleagues reviewed the vibration and nonlinear dynamic response of imperfect sandwich piezoelectric auxetic plates [8] . Li and Cheng provided a method, known as the differential quadrature technique, for studying the nonlinear vibration of orthotropic plates considering transverse shear effect and finite deformation [9]. These researchers evaluated nonlinear free vibration behavior using differential quadrature method and employed the harmonic balance process for deriving motion relations. Lal and others conducted the nonlinear free vibration analysis of laminated composite plates on an elastic foundation with random system features[10] . They obtained characteristic numerical findings (second-order statistics) for composite plates supported by Winkler and Pasternak elastic foundations under varying support conditions. The problem's formulation was based on a higher-order shear displacement theory, encompassing rotatory inertia impacts and von Karman-type nonlinear strain displacement relations. Using a C^0 finite element approach, the laminate was discretized. They devised an iterative approach along with a perturbation technique based on first-order Taylor series to address the random nonlinear generalized eigenvalue problem. Tian et al. proposed a fresh higher-order approach for sandwich plates featuring a elastic core[11] . Malekzadeh and colleagues studied the dynamic reaction of in-plane pre-stressed sandwich panels incorporating a viscoelastic flexible core and various boundary conditions[12] .

Utilizing conventional theories for moderately thick laminated plates might yield inaccurate information. In anisotropic materials, there's an interplay between bending and stretching of laminated composite plates for overlooking shear strains and rotary inertia effects. Therefore, the FSDT and higher-order SDT theories were both utilized to analyze the nonlinear vibration behavior of these laminated plates. Frostig [13] formulated an advanced theory for sandwich panels with higher-order considerations. Malekzadeh et al. [14] presented an enhanced higher-order theory for sandwich plates by integrating the FSDT theory into the face sheets. Smart fluids and elastomers, featuring variable stiffness and damping features, capable of adjusting their rheology in reaction to an imposed electric or magnetic field, present promising opportunities for creating adaptive sandwich configurations with superior vibration damping across a broad frequency spectrum. Eshaghi et al. [15] investigated the dynamic traits and control mechanisms of electrorheological or magnetorheological sandwich constructions. Carlson [16] initially introduced the principles behind ER(ElectroRheological) adaptive structures employing materials. Yeh and Chen conducted an exploration into the dynamic stability issues of an ER(ElectroRheological) sandwich beam and elucidated dynamic characteristics of several types of sandwich plates—such as orthotropic, annular, orthotropic annular, and rotating polar orthotropic annular ones—by varying ER layer thickness and electric field strength[17-22]. Keshavarzian et al. examined the high-order linear vibration characteristics of a moderately thick sandwich panel featuring an ER core[23] . Additionally, their research involved investigating the nonlinear free vibration analysis of a thick sandwich panel equipped with an electrorheological core [24]. They also explored applying smart magnetorheological and electrorheological fluid cores in dampening vibration behavior of sandwich panels, by the use of an innovative HSDT theory [25]. Nayak et al. dynamically analyzed a sandwich beam utilizing magnetorheological elastomer with conductive skins, exploring varying boundary situations[26] . Meanwhile, Yu-Hang Li et al. investigated the dynamic characteristics of a rectangular plate comprising a magnetorheological fluid core and a constraining layer[27] . They established mathematical models using the finite element approach and assessed the impact of various magnetic field intensities and various thicknesses of the MR layer on frequency and loss factor. Their results demonstrated that as the magnetic field intensity increased, the frequency heightened while the loss factor diminished. On the contrary, elevating the thickness of the MR layer resulted in an initial frequency decrease, succeeded by a swift rise, alongside a consistent increase in the loss factor.

There is a scarcity of published research focusing on nonlinear vibration characteristics of sandwich panels featuring MR fluid cores, despite the numerous studies performed on vibration behavior of such panels. Consequently, additional research is undoubtedly necessary to elucidate this subject further.

This research aimed to establish the nonlinear equations of motion in sandwich panels comprising multiple face sheets and an MR fluid core, considering the mentioned information. To achieve this, we utilized the New Sinusoidal Shear Deformation Theory, accounting for rotary inertia.

We aimed to evaluate dynamic characteristics of these sandwich panels using Galerkin's approach, focusing on aspects such as the geometric aspect ratio, magnetic field strength, and thickness of the MR core layer. Upon presenting a force function, these relations were condensed into several coupled nonlinear partial differential equations (PDEs) along with a compatibility equation. We validated the accuracy of our study initially on isotropic materials and then expanded our investigation to laminated rectangular panels, analyzing the nonlinear free vibration patterns of the panel.

Furthermore, the influence of system parameters on frequency of nonlinear vibration was evaluated.

2. THEORETICAL FORMULATION

2.1. Elementary Assumptions

The fundamental premise entailed a thick composite sandwich panel including a core layer and two laminated face sheets, where the top and bottom cover thickness, as well as the core material, were specified: [redacted]. The suggested sandwich panel would possess dimensions: a length of "a," a width of "b," and an overall thickness of "h." Besides, Figure 1indicates the orthogonal coordinates [redacted]. Where, the "*t"* index denotes the upper sheet, "b" is the lower sheet, and "c" shows the core.

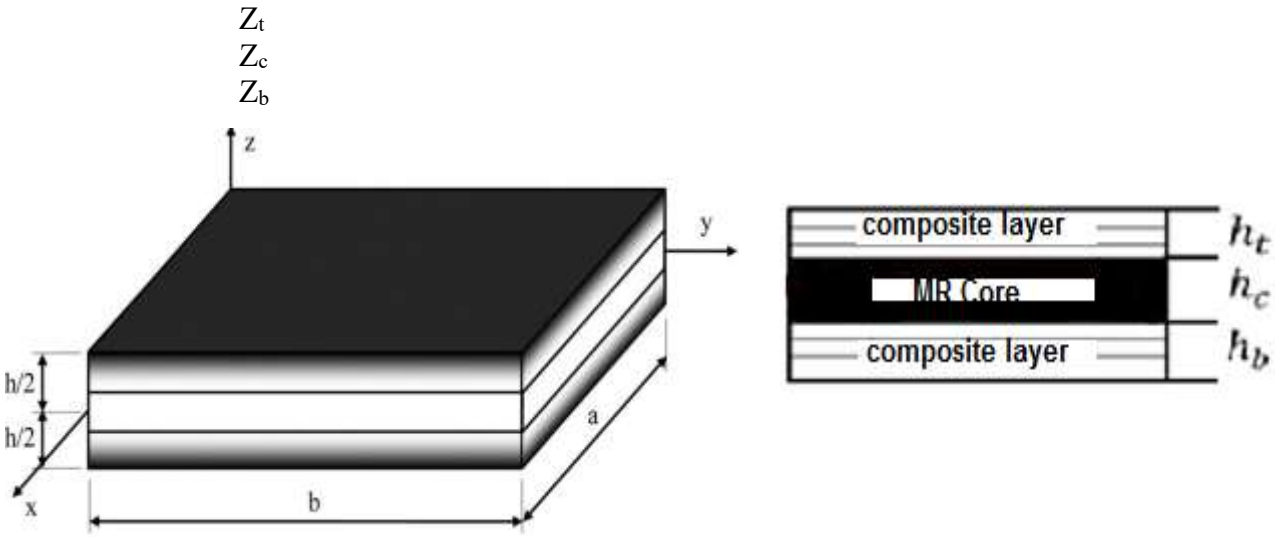

Figure 1. A sandwich panel featuring laminated face sheets, an MR core, and orthogonal coordinates

2.2. Formulations

2.2.1 Displacement field model

Within the Higher-order Shear Deformation Theory (HSDT), the displacement field can be articulated as:

$$u_i(x,z,y,t) = u_0^i(x,y,t) + f_1(z_i)\frac{\partial w_0(x,y,t)}{\partial x} + f_2(z_i)\phi_x^i(x,y,t)$$

$$v_i(x,z,y,t) = v_0^i(x,y,t) + f_1(z_i)\frac{\partial w_0(x,y,t)}{\partial y} + f_2(z_i)\phi_y^i(x,y,t) \quad ; \quad (i = t,b) \tag{1}$$

$$w_i(x,z,y,t) = w_0^i(x,y,t)$$

where u_i, v_i and w_i show the point displacements along the (x, y, z) coordinates. u_0^i, v_i and w_0^i correspond the point displacements on the mid plane. ϕ_x^i and ϕ_y^i denote the rotations of normal to the mid plane about the y- and x-axis.
According to table 1, it is possible to easily obtain The plate theories through changing the functions $f_1(z_i), f_2(z_i)$.

Table 1. different shear deformation Theories

plate theories	$f_1(z)$	$f_2(z)$
Classic [28]	$-z$	0
First- order [28]	0	z

Third- order [28]	$-\frac{4}{3h^2}z^3$	$z-\frac{4}{3h^2}z^3$
exponential [29]	$-z$	$ze^{-2\left(\frac{z}{h}\right)^2}$
trigonometric [30]	$-z$	$\frac{h}{\pi}sin\left(\frac{\pi z}{h}\right)$
hyperbolic [31]	$-z$	$hsinh\left(\frac{z}{h}\right)-zcosh\left(\frac{1}{2}\right)$
parabolic [32]	$-z$	$z\left(\frac{5}{4}-\frac{5}{3h^2}z^2\right)$
1st suggestion	$-z$	$z\left(\frac{3}{h}-\frac{4}{h^3}z^2\right)$
2st suggestion	$-z$	$z\left(\frac{1}{h}-\frac{2}{h^3}z^2+\frac{8}{5h^5}z^4\right)$
new higher- order shear deformation theory [33]	$-z$	$\frac{h}{\pi}sin\left(\frac{\pi z}{h}\right)\left(e^{\frac{1}{2}cos\left(\frac{\pi z}{h}\right)}+1\right)-z\left(\frac{1}{2}-\frac{4z^2}{3h^2}\right)$

2.2.2. classical laminated plate theory (CLPT)

The most basic Equivalent Single Layer (ESL) laminated plate theory is known as the CLPT. According to the displacement field, lines vertical to the xy-plane pre-deformation remain perpendicular and straight in relation to the mid-surface post-deformation. The Kirchhoff assumption involves disregarding both transverse shear and transverse normal effects. Consequently, the deformation solely arises from bending and in-plane stretching [28].

2.2.3. First-order of Laminated Composite Plates

The First-order Shear Deformation Theory (FSDT) expands upon the kinematics of the CLPT by incorporating significant transverse shear deformation in its assumptions. Here, the transverse shear strain is considered constant concerning the thickness coordinate. This inclusion of basic shear deformation relaxes the normality constraints of the classical laminate theory. However, the FSDT introduces shear correction factors, which pose challenges in determining them for arbitrarily laminated composite plate structures. These correction factors are not solely reliant on lamination and geometric factors; they hinge on the imposed boundary and loading conditions [28].

2.2.4. Third-Order Theory of Laminated Composite Plates

The forthcoming third-order plate theory, like the classic and first-order plate theories, follows similar assumptions. However, it deviates by relaxing the assumption regarding the linearity and perpendicularity of a transverse normal post-deformation. This is achieved by expanding the displacements u, v, and w as cubic functions concerning the thickness coordinate. In Figure 1, the deformation kinematics of a transverse normal at the edge (y = 0) are depicted [28].

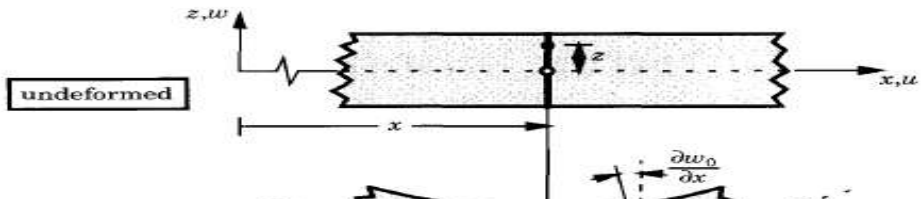

Figure 2. A transverse normal deformation based on the first-order, third-order, and classical plate theories [28]

2.2.5. Exponential Shear Deformation Theory

Within this theory, the in-plane displacement u along the x-direction and v along the y-direction comprise two elements:
(a) A displacement element akin to the classical plate theory of bending.
(b) A displacement element attributed to shear deformation, expected to exhibit an exponential nature concerning the thickness coordinate.The exponential function, represented as $f_2(z)$ with regards to the thickness coordinate, impacts both the in-plane displacements u and v, correlating with the distribution of transverse shear stress across The plate thickness. The Exponential Shear Deformation Theory stands as a refined, displacement-based theory, acknowledged for its effectiveness in enhancing the precision of displacements and stress assessments. The kinematic framework within this theory exceeds the complexity of HSDTs in existing literature. This is primarily because, upon expanding the exponential term into a power series, the kinematic characteristics of higher-order theories are significantly considered. Unlike the sine function that encompasses solely odd powers, the exponential function incorporates both even and odd powers within its expansion[29] .

2.2.6. New Higher- Order Shear Deformation Theory

This novel HSDT utilizes a set of shape functions that combine trigonometric, polynomial, and exponential functions, in contrast to the traditional use of only polynomial functions. The selected shape function aims to precisely represent the distribution of shear deformation throughout The plate thickness. Furthermore, this proposed shape function fulfills the conditions of zero shear stress on both the lower and upper surfaces of The plate, eliminating the need for considering shear correction factors [30].

2.2.7. New Sinusoidal Shear Deformation theory

In the present work, a fresh sinusoidal shear deformation theory was introduced to examine the Large Amplitude Free Vibration of thick Laminated Composite Plates equipped with a Magnetorheological Core. This theory incorporated an undefined integral term to minimize the unknowns to just four, eliminating the need for shear correction factors. The efficacy and precision of this theory were validated through comparisons with existing solutions, affirming its high accuracy and efficiency.

We define ϕ_x^i and ϕ_y^i as follows:

$$\phi_x^i(x,y,t) = \left(\frac{\partial\theta^i(x,y,t)}{\partial x} + \frac{\partial w_0^i(x,y,t)}{\partial x}\right) \tag{2}$$

$$\phi_y^i(x,y,t) = \left(\frac{\partial\theta^i(x,y,t)}{\partial y} + \frac{\partial w_0^i(x,y,t)}{\partial y}\right)$$

The proposed shear deformation theory introduces two derivative quantities, $\frac{\partial\theta(x,y,t)}{\partial x}$ and $\frac{\partial\theta(x,y,t)}{\partial y}$, resulting in only four unknown displacement functions. This approach reduces the number of unknowns compared to other Higher-order Shear Deformation Theories (HSDTs), which typically involve five to eight unknowns, thereby potentially lowering computational costs [31].In this investigation, an innovative sinusoidal shear deformation theory is derived by establishing the following conditions:

$$f_1(z_i) = z \ , f_2(z) = \frac{h\sqrt{15}}{3\pi} sin\left(\frac{\pi z}{h}\right) \tag{3}$$

The innovative sinusoidal shear deformation theory meets requirements of The plate shear strains and stresses. The shear stress distribution must be parabolical over The plate thickness as the first condition. The second requirement is that the shear stresses and strains must be zero at all points on The plate free surfaces. Consequently, the proposed theory doesn't require shear correction factors, in contrast to FSDTs. Here, z_i represents the vertical coordinate of face sheets (i = t, b), measured upward from the mid-plane of each face sheet The relations describing the movement of the face sheets are:[32]

$$\varepsilon_{xx}^i = \varepsilon_{0xx}^i + f_1(z)L_{xx}^i + f_2(z)k_{xx}^i \ , \ \varepsilon_{yy}^i = \varepsilon_{0yy}^i + f_1(z)L_{yy}^i + f_2(z)k_{yy}^i \ , \varepsilon_{zz}^i = 0$$

$$\gamma_{xy}^i = 2\varepsilon_{xy}^i = \gamma_{0xy}^i + f_1(z)L_{xy}^i + f_2(z)k_{xy}^i$$

$$\gamma_{xz}^i = 2\varepsilon_{xz}^i = \gamma_{0xz}^i + \frac{\partial f_1(z)}{\partial z_i}G_{xz}^i + \frac{\partial f_2(z)}{\partial z_i}T_{xz}^i, \qquad ؛ \qquad (i = t, b) \tag{4}$$

$$\gamma_{yz}^i = 2\varepsilon_{yz}^i = \gamma_{0yz}^i + \frac{\partial f_1(z)}{\partial z_i}G_{yz}^i + \frac{\partial f_2(z)}{\partial z_i}T_{yz}^i$$

Where,

$$\varepsilon_{0xx}^i = \frac{\partial u_0^i}{\partial x} + \frac{1}{2}\left(\frac{\partial w_0^i}{\partial x}\right)^2, \quad \varepsilon_{0yy}^i = \frac{\partial v_0^i}{\partial y} + \frac{1}{2}\left(\frac{\partial w_0^i}{\partial y}\right)^2 \ , \gamma_{0xy}^i = \frac{\partial v_0^i}{\partial x} + \frac{\partial u_0^i}{\partial y} + \frac{\partial w_0^i}{\partial x}\ \frac{\partial w_0^i}{\partial y}$$

$$\gamma_{0xz}^i = \frac{\partial w_0^i}{\partial x} \ , \ \gamma_{0yz}^i = \frac{\partial w_0^i}{\partial y} \ , \ L_{xx}^i = \frac{\partial^2 w_0^i}{\partial x^2}, \quad k_{xx}^i = \frac{\partial \phi_x^i}{\partial x}, \ L_{yy}^i = \frac{\partial^2 w_0^i}{\partial y^2}, \quad k_{yy}^i = \frac{\partial \phi_y^i}{\partial y}, \tag{5}$$

$$L_{xy}^i = 2\frac{\partial^2 W_0^i}{\partial x \partial y}, \quad k_{xy}^i = \frac{\partial \phi_x^i}{\partial y} + \frac{\partial \phi_y^i}{\partial x} \ , \ G_{xz}^i = \frac{\partial w_0^i}{\partial x} \ , T_{xz}^i = \phi_x^i \ , G_{yz}^i = \frac{\partial w_0^i}{\partial y} \ , T_{yz}^i = \phi_y^i$$

2.3. Displacement field for the thick core layer:

$$u_c(x, y, z, t) = u_0^c(x, y, t) + z_c u_1^c(x, y, t) + z_c^2 u_2^c(x, y, t) + z_c^3 u_3^c(x, y, t),$$

$$v_c(x, y, z, t) = v_0^c(x, y, t) + z_c v_1^c(x, y, t) + z_c^2 v_2^c(x, y, t) + z_c^3 v_3^c(x, y, t), \tag{6}$$

$$w_c(x, y, z, t) = w_0^c(x, y, t) + z_c w_1^c(x, y, t) + z_c^2 w_2^c(x, y, t).$$

The kinematic connections governing the behavior of the core layer are:

$\varepsilon_{xx}^{c} = \frac{\partial u_c}{\partial x}, \varepsilon_{yy}^{c} = \frac{\partial v_c}{\partial y}, \varepsilon_{zz}^{c} = \frac{\partial w_c}{\partial z}$

$$\gamma_{xy}^{c} = 2\varepsilon_{xy}^{c} = \frac{\partial v_c}{\partial x} + \frac{\partial u_c}{\partial y} \quad , \quad \gamma_{xz}^{c} = 2\varepsilon_{xz}^{c} = \frac{\partial w_c}{\partial x} + \frac{\partial u_c}{\partial z} \quad , \quad \gamma_{yz}^{c} = 2\varepsilon_{yz}^{c} = \frac{\partial w_c}{\partial y} + \frac{\partial v_c}{\partial z} \tag{7}$$

The strains can be derived in relation to the displacement of the mid-plane by inserting equation (6) into relations (7), resulting in the following outcome:

$$\varepsilon_{xx}^{c} = (\varepsilon_{0xx} + z_c x_{0xx} + {z_c}^2 \varepsilon_{0xx}^{*} + {z_c}^3 x_{0xx}^{*}) \, , \varepsilon_{yy}^{c} = \left(\varepsilon_{0yy} + z_c x_{0yy} + {z_c}^2 \varepsilon_{0yy}^{*} + {z_c}^3 x_{0yy}^{*}\right)$$

$$\varepsilon_{zz}^{c} = \varepsilon_{0zz} + z_c x_{0zz}$$

$$\gamma_{xy}^{c} = \varepsilon_{0xy} + z_c x_{0xy} + {z_c}^2 \varepsilon_{0xy}^{*} + {z_c}^3 x_{0xy}^{*} + \varepsilon_{0yx} + z_c x_{0yx} + {z_c}^2 \varepsilon_{0yx}^{*} + {z_c}^3 x_{0yx}^{*} \tag{8}$$

$$\gamma_{xz}^{c} = \varepsilon_{0xz} + z_c x_{0xz} + {z_c}^2 \varepsilon_{0xz}^{*} + {z_c}^3 x_{0xz}^{*} + \varepsilon_{1xz} + z_c x_{1xz} + {z_c}^2 \varepsilon_{1xz}^{*}$$

$$\gamma_{yz}^{c} = \varepsilon_{0yz} + z_c x_{0yz} + {z_c}^2 \varepsilon_{0yz}^{*} + {z_c}^3 x_{0yz}^{*} + \varepsilon_{1yz} + z_c x_{1yz} + {z_c}^2 \varepsilon_{1yz}^{*}$$

Where:

$$\varepsilon_{0xx} = \frac{\partial u_0^c}{\partial x}, \quad \chi_{0xx} = \frac{\partial u_1^c}{\partial x} \quad , \varepsilon_{0xx}^{*} = \frac{\partial u_2^c}{\partial x}, \quad \chi_{0xx}^{*} = \frac{\partial u_3^c}{\partial x} \, , \varepsilon_{0yy} = \frac{\partial v_0^c}{\partial y},$$

$$\chi_{0yy} = \frac{\partial v_1^c}{\partial y} \quad , \varepsilon_{0yy}^{*} = \frac{\partial v_2^c}{\partial y}, \quad \chi_{0yy}^{*} = \frac{\partial v_3^c}{\partial y} \, , \varepsilon_{0zz} = w_1^c, \quad \chi_{0zz} = 2w_2^c$$

$$\varepsilon_{0xy} = \frac{\partial v_0^c}{\partial x} \, , \chi_{0xy} = \frac{\partial v_1^c}{\partial x} \, , \quad \varepsilon_{0xy}^{*} = \frac{\partial v_2^c}{\partial x} \, , \quad \chi_{0xy}^{*} = \frac{\partial v_3^c}{\partial x} \, , \varepsilon_{0yx} = \frac{\partial u_0^c}{\partial y} \, , \quad \chi_{0yx} = \frac{\partial u_1^c}{\partial y} \tag{9}$$

$$\varepsilon_{0yx}^{*} = \frac{\partial u_2^c}{\partial y} \, , \quad \chi_{0yx}^{*} = \frac{\partial u_3^c}{\partial y} \, , \varepsilon_{0xz} = \frac{\partial w_0^c}{\partial x} \, , \quad \chi_{0xz} = \frac{\partial w_1^c}{\partial x} \, , \quad \varepsilon_{0xz}^{*} = \frac{\partial w_2^c}{\partial x} \, , \chi_{0xz}^{*} = 0$$

$$\varepsilon_{1xz} = u_1^c \, , \quad \chi_{1xz} = 2u_2^c \, , \quad \varepsilon_{xz}^{*} = 3u_3^c \quad \varepsilon_{0yz} = \frac{\partial w_0^c}{\partial y} \, , \quad \chi_{0yz} = \frac{\partial w_1^c}{\partial y} \, , \quad \varepsilon_{0yz}^{*} = \frac{\partial w_2^c}{\partial y}$$

$$\chi_{0xy}^{*} = 0 \, , \quad \varepsilon_{1yz} = v_1^c \, , \quad \chi_{1yz} = 2v_2^c \, , \quad \varepsilon_{yz}^{*} = 3v_3^c$$

If the bottom and top face sheets and core interfaces are bonded perfectly, the following compatibility conditions are obtained:

$$\begin{cases} u_c(z = z_{ci}) = u_0^i + \frac{1}{2}(-1)^k h_i \phi_x^i \\ v_c(z = z_{ci}) = v_0^i + \frac{1}{2}(-1)^k h_i \phi_y^i \\ w_c(z = z_{ci}) = w_0^i \end{cases} \quad \begin{cases} For \; i = t \rightarrow \left(k = 1 ; z_{ct} = \frac{h_c}{2}\right) \\ For \; i = b \rightarrow \left(k = 0 ; z_{cb} = -\frac{h_c}{2}\right) \end{cases} \tag{10}$$

Using (4) and (6) and simplifying, the compatibility conditions is represented as below:

$$u_2^c = \frac{2(u_0^t+u_0^b)-h_t\phi_x^t+h_b\phi_x^b-4u_0^c}{h_c^2}\ , u_3^c = \frac{4(u_0^t-u_0^b)-2(h_t\phi_x^t+h_b\phi_x^b)-4h_cu_1^c}{h_c^3}$$

$$v_2^c = \frac{2(v_0^t+v_0^b)-h_t\phi_y^t+h_b\phi_y^b-4v_0^c}{h_c^2}\ , v_3^c = \frac{4(v_0^t-v_0^b)-2(h_t\phi_y^t+h_b\phi_y^b)-4h_cv_1^c}{h_c^3} \quad (11)$$

$$w_1^c = \frac{(w_0^t+w_0^b)}{h_c}\ , w_2^c = \frac{2(w_0^t+w_0^b)-4w_0^c}{h_c^2}$$

According to (11), there are five unknown elements in the core layer: [redacted] and [redacted] . Thus, the unknowns for a flat composite sandwich panel includes 15 items:

$$\{u_0^t\ , v_0^t, w_0^t, \psi_x^t, \psi_y^t, u_0^b, v_0^b, w_0^b, \psi_x^b, \psi_y^b, u_0^c\ , u_1^c, v_0^c\ , v_1^c, w_0^c\}$$

2.4. The stress resultants for the core

The stress impacts the core in the this manner:

$$\begin{Bmatrix} N_{xx}^c \\ N_{yy}^c \\ N_{xy}^c \end{Bmatrix} = \int_{-h_c/2}^{h_c/2} \begin{Bmatrix} \sigma_{xx}^c \\ \sigma_{yy}^c \\ \sigma_{xy}^c \end{Bmatrix} dz_c\ , \begin{Bmatrix} M_{nxx}^c \\ M_{nyy}^c \\ M_{nxy}^c \end{Bmatrix} = \int_{-h_c/2}^{h_c/2} z_c^n \begin{Bmatrix} \sigma_{xx}^c \\ \sigma_{yy}^c \\ \sigma_{xy}^c \end{Bmatrix} dz_c, \begin{Bmatrix} N_{xz}^c \\ N_{yz}^c \\ M_{nxz}^c \\ M_{nyz}^c \end{Bmatrix} = \int_{-h_c/2}^{h_c/2} z_c^n \begin{Bmatrix} \sigma_{xz}^c \\ \sigma_{yz}^c \\ z_c^n\sigma_{xz}^c \\ z_c^n\sigma_{yz}^c \end{Bmatrix} dz_c \quad (12)$$

$$\{R_z^c, M_z^c\} = \int_{-h_c/2}^{h_c/2} (1, z_c)\sigma_{zz}^c dz_c\ , \qquad n = 1,2,3$$

2.5. Resulting stress per unit length of the face sheets

The resultant stress per unit length of the face sheets is described as:

$$\begin{Bmatrix} N_{xx}^i \\ N_{yy}^i \\ N_{xy}^i \end{Bmatrix} = \int_{-h_i/2}^{h_i/2} \begin{Bmatrix} \sigma_{xx}^i \\ \sigma_{yy}^i \\ \sigma_{xy}^i \end{Bmatrix} dz\ , \begin{Bmatrix} M_{xx}^i \\ M_{yy}^i \\ M_{xy}^i \end{Bmatrix} = \int_{-h_i/2}^{h_i/2} f_1(z) \begin{Bmatrix} \sigma_{xx}^i \\ \sigma_{yy}^i \\ \sigma_{xy}^i \end{Bmatrix} dz\ , \begin{Bmatrix} P_{xx}^i \\ P_{yy}^i \\ P_{xy}^i \end{Bmatrix} = \int_{-h_i/2}^{h_i/2} f_2(z) \begin{Bmatrix} \sigma_{xx}^i \\ \sigma_{yy}^i \\ \sigma_{xy}^i \end{Bmatrix} dz$$

$$N_{xz}^i = \int_{-h_i/2}^{h_i/2} \sigma_{xz}^i dz\ , R_{xz}^i = \int_{-h_i/2}^{h_i/2} \left(\frac{df_1(z)}{dz}\right) \sigma_{xz}^i dz, S_{xz}^i = \int_{-h_i/2}^{h_i/2} \left(\frac{df_2(z)}{dz}\right) \sigma_{xz}^i dz,\ i = t, b \quad (13)$$

$$N_{yz}^i = \int_{-h_i/2}^{h_i/2} \sigma_{yz}^i dz\ , R_{yz}^i = \int_{-h_i/2}^{h_i/2} \left(\frac{df_1(z)}{dz}\right) \sigma_{yz}^i dz, S_{yz}^i = \int_{-h_i/2}^{h_i/2} \left(\frac{df_2(z)}{dz}\right) \sigma_{yz}^i dz,\ i = t, b$$

2.6. Equations of Motion

The sandwich panel motion relations were obtained by Hamilton's approach.
It is presented analytically as:

$$\int_0^t \delta L dt = \int_0^t (\delta K - \delta U + \delta W_{ext}) dt = 0 \quad (14)$$

Where, [redacted] *and* [redacted] present strain and kinetic energy variations. Besides, δW_{ext} potential energy variation is produced by external forces and "t" denotes the duration between "t_1 and t_2" times, and "[redacted]" shows the variation operator. Therefore, the primary variation equation of kinetic energy (assuming uniform conditions for displacement and velocity regarding time) is:

$$\delta K = -\sum_{i=t,b,c}\left[\iint_{A_i}\int_{-h_i/2}^{h_i/2}\rho_i(\ddot{u}_i\delta u_i + \ddot{v}_i\delta v_i + \ddot{w}_i\delta w_i)dz_i\, dA_i\right] \quad (15)$$

$$dA_c = dx_c dy_c, \quad dA_i = dx_i dy_i, \quad (i = t, b)$$

The sandwich panel cases and total strain energy of the core are stated as follows:

$$\delta U = \sum_{i=t,b}\left(\int_{V_i}\left(\sigma_{xx}^i\delta\varepsilon_{xx}^i + \sigma_{yy}^i\delta\varepsilon_{yy}^i + \gamma_{xy}^i\delta\gamma_{xy}^i + \gamma_{xz}^i\delta\gamma_{xz}^i + \gamma_{yz}^i\delta\gamma_{yz}^i\right)dV_i\right)$$

$$+\int_{V_c}\left(\sigma_{xx}^c\delta\varepsilon_{xx}^c + \sigma_{yy}^c\delta\varepsilon_{yy}^c + \gamma_{xy}^c\delta\gamma_{xy}^c + \gamma_{xz}^c\delta\gamma_{xz}^c + \gamma_{yz}^c\delta\gamma_{yz}^c\right)dV_c \quad (16)$$

Where: $dV_c = dA_c dZ_c = dx_c dy_c dz_c$, $dV_i = dA_i dz_i = dx_i dy_i dz_i$; $(i = t, b)$

Ultimately, we must replace the kinetic energy fluctuations and system potentials with relations of strain-displacement and displacement fields. The motion equations are discovered by using the Hamilton's principle. Only one equation is used as an example due to the lengthy equations:

δu_0^t:

$$\frac{\partial N_{xx}^t}{\partial x} + \frac{\partial N_{xy}^t}{\partial y} + \frac{2}{h_C^2}\frac{\partial M_{2xx}^C}{\partial x} + \frac{4}{h_C^3}\frac{\partial M_{3xy}^C}{\partial y} + \frac{2}{h_C^2}\frac{\partial M_{2xy}^C}{\partial y} - \frac{4M_{1xz}^C}{h_C^2} - \frac{12M_{2xz}^C}{h_C^3} + \frac{4}{h_C^3}\frac{\partial M_{3xx}^C}{\partial x} = \quad (17)$$

$$\left(-\frac{16I_5^c}{h_c^5} - \frac{8I_4^C}{h_c^4} + \frac{4I_3^C}{h_c^3} + \frac{2I_2^C}{h_c^2}\right)\ddot{u}_0^C + \left(\frac{2I_3^C}{h_c^2} - \frac{8I_5^C}{h_c^4} - \frac{16I_6^C}{h_c^5} + \frac{4I_4^C}{h_c^3}\right)\ddot{u}_1^C + \left(\frac{4I_4^C}{h_c^4} - \frac{16I_6^C}{h_c^6}\right)\ddot{u}_0^b + \left(\frac{16I_6^C}{h_c^6} + \frac{4I_4^C}{h_c^4} + \frac{16I_5^C}{h_c^5} + I_0^t\right)\ddot{u}_0^t$$

$$+\left(\frac{2I_4^C h_b}{h_c^4} - \frac{8h_b I_6^C}{h_c^6}\right)\ddot{\emptyset}_x^b + \left(-\frac{8h_t I_5^C}{h_c^5} + I_2^t - \frac{2I_4^C h_t}{h_c^4} - \frac{8h_t I_6^C}{h_c^6}\right)\ddot{\emptyset}_x^t + I_1^t\ddot{W}_{0,x}^t$$

The core's moment of inertia is defined through the subsequent equations[35] :

$$I_n^c = \int_{-\frac{h_c}{2}}^{\frac{h_c}{2}}\rho_c z_c^n\, dz_c \qquad n = 0,1,\ldots,6 \quad (18)$$

Additionally, the inertia moment of the face sheets is deduced from the following equations:

$$I_0^t = \int_{-\frac{h_t}{2}}^{\frac{h_t}{2}}\rho_t\, dz_t\,, I_1^t = \int_{-\frac{h_t}{2}}^{\frac{h_t}{2}}\rho_t f_1(z)dz_t\,, I_2^t = \int_{-\frac{h_t}{2}}^{\frac{h_t}{2}}\rho_t f_2(z)dz_t\,, I_3^t = \int_{-\frac{h_t}{2}}^{\frac{h_t}{2}}\rho_t f_1(z)f_2(z)dz_t \quad (19)$$

$$I_4^t = \int_{-\frac{h_t}{2}}^{\frac{h_t}{2}}\rho_t\,[f_2(z_i)]^2 dz_t$$

$$I_0^b = \int_{-\frac{h_b}{2}}^{\frac{h_b}{2}}\rho_b\, dz_b\,, I_1^b = \int_{-\frac{h_b}{2}}^{\frac{h_b}{2}}\rho_b f_1(z)dz_b\,, I_2^b = \int_{-\frac{h_b}{2}}^{\frac{h_b}{2}}\rho_b f_2(z)dz_b, I_3^b = \int_{-\frac{h_b}{2}}^{\frac{h_b}{2}}\rho_b f_1(z)f_2(z)dz_b$$

$$, I_4^b = \int_{-\frac{h_b}{2}}^{\frac{h_b}{2}} \rho_b \, [f_2(z)]^2 dz_b$$

2.7. Lamina Constitutive Relations

2.7.1. Lamina Constitutive Relations for face sheets

The linear constitutive relations in the principal material coordinates for the k[th] orthotropic lamina are as below:

$$\begin{bmatrix}\sigma_{xx}\\ \sigma_{yy}\\ \sigma_{xy}\end{bmatrix} = \begin{bmatrix}\mathrm{Q}_{11} & \mathrm{Q}_{12} & \mathrm{Q}_{16}\\ \mathrm{Q}_{12} & \mathrm{Q}_{22} & \mathrm{Q}_{26}\\ \mathrm{Q}_{16} & \mathrm{Q}_{26} & \mathrm{Q}_{66}\end{bmatrix}^{(k)} \begin{bmatrix}\varepsilon_{xx}\\ \varepsilon_{yy}\\ \varepsilon_{xy}\end{bmatrix} \quad , \begin{bmatrix}\sigma_{yz}\\ \sigma_{xz}\end{bmatrix} = \begin{bmatrix}\mathrm{Q}_{44} & \mathrm{Q}_{45}\\ \mathrm{Q}_{45} & \mathrm{Q}_{55}\end{bmatrix}^{(k)} \begin{bmatrix}\varepsilon_{yz}\\ \varepsilon_{xz}\end{bmatrix} \tag{20}$$

Where $Q_{ij}^{(k)}$ denotes the plane stress-reduced stiffness. Also, for Q_{ij} of each layer, (19) is present:

$$Q_{11} = \frac{E_1}{1-v_{12}v_{21}}, Q_{12} = \frac{v_{12}E_1}{1-v_{12}v_{21}}, Q_{22} = \frac{E_2}{1-v_{12}v_{21}} \ , Q_{66} = G_{12}, Q_{44} = G_{23}, Q_{55} = G_{13} \tag{21}$$

2.7.2. Lamina Constitutive Relations for the core material

Hooke's Law expressions for the core layer are stated as:

$$\sigma_{xx}^C = E_{xx}^C(z)\epsilon_{xx}^C = E_{xx}^C(z)\left(\left(\frac{\partial u_0^c}{\partial x} + z_c\frac{\partial u_1^c}{\partial x} + {z_c}^2\frac{\partial u_2^c}{\partial x} + {z_c}^3\frac{\partial u_3^c}{\partial x}\right)\right)$$

$$\sigma_{yy}^C = E_{yy}^C(z)\epsilon_{yy}^C = E_{yy}^C(z)\left(\left(\frac{\partial v_0^c}{\partial y} + z_c\frac{\partial v_1^c}{\partial y} + {z_c}^2\frac{\partial v_2^c}{\partial y} + {z_c}^3\frac{\partial v_3^c}{\partial y}\right)\right)$$

$$\sigma_{zz}^C = E_{zz}^C(z)\epsilon_{zz}^C = E_{zz}^C(z)\left(\frac{\partial w_c}{\partial z}\right) = E_{zz}^C(z)(w_1^c + z_c 2w_2^c) \tag{22}$$

$$\sigma_{xy}^C = G_{xy}^C(z)\gamma_{xy}^C = G_{xy}^C(z)\left(\left(\frac{\partial v_0^c}{\partial x} + z_c\frac{\partial v_1^c}{\partial x} + {z_c}^2\frac{\partial v_2^c}{\partial x} + {z_c}^3\frac{\partial v_3^c}{\partial x} + \frac{\partial u_0^c}{\partial y} + z_c\frac{\partial u_1^c}{\partial y} + {z_c}^2\frac{\partial u_2^c}{\partial y} + {z_c}^3\frac{\partial u_3^c}{\partial y}\right)\right)$$

$$\sigma_{xz}^C = G_{xz}^C(z)\gamma_{xz}^C = G_{xz}^C(z)\left(\frac{\partial w_c}{\partial x} + \frac{\partial u_c}{\partial z}\right) = G_{xz}^C(z)\left(\frac{\partial w_0^c}{\partial x} + z_c\frac{\partial w_1^c}{\partial x} + {z_c}^2\frac{\partial w_2^c}{\partial x} + u_1^c + z_c 2u_2^c + {z_c}^2 3u_3^c\right)$$

$$\sigma_{yz}^C = G_{yz}^C(z)\gamma_{yz}^C = G_{yz}^C(z)\left(\frac{\partial w_c}{\partial y} + \frac{\partial v_c}{\partial z}\right) = G_{yz}^C(z)\left(\frac{\partial w_0^c}{\partial y} + z_c\frac{\partial w_1^c}{\partial y} + {z_c}^2\frac{\partial w_2^c}{\partial y} + v_1^c + z_c 2v_2^c + {z_c}^2 3v_3^c\right)$$

Stress resultants per unit length for the core layer are stated as follows:

$$N_{xx}^C = \int_{-\frac{h_c}{2}}^{\frac{h_c}{2}} \sigma_{xx}^c \, dz_c = \int_{-\frac{h_c}{2}}^{\frac{h_c}{2}} E_{xx}^c(Z)\left(\left(\frac{\partial u_0^c}{\partial x} + z_c\frac{\partial u_1^c}{\partial x} + {z_c}^2\frac{\partial u_2^c}{\partial x} + {z_c}^3\frac{\partial u_3^c}{\partial x}\right)\right)dz_c$$

$$N_{yy}^{C}=\int_{-\frac{h_c}{2}}^{\frac{h_c}{2}}\sigma_{yy}^{c}\,dz_c=\int_{-\frac{h_c}{2}}^{\frac{h_c}{2}}E_{yy}^{c}\,(Z)\left(\left(\frac{\partial v_0^c}{\partial y}+z_c\frac{\partial v_1^c}{\partial y}+{z_c}^2\frac{\partial v_2^c}{\partial y}+{z_c}^3\frac{\partial v_3^c}{\partial y}\right)\right)dz_c$$

$$N_{xy}^{C}=\int_{-\frac{h_c}{2}}^{\frac{h_c}{2}}\sigma_{xy}^{c}\,dz_c=\int_{-\frac{h_c}{2}}^{\frac{h_c}{2}}G_{xy}^{c}(z)\left(\left(\frac{\partial v_0^c}{\partial x}+z_c\frac{\partial v_1^c}{\partial x}+{z_c}^2\frac{\partial v_2^c}{\partial x}+{z_c}^3\frac{\partial v_3^c}{\partial x}+\frac{\partial u_0^c}{\partial y}+z_c\frac{\partial u_1^c}{\partial y}+{z_c}^2\frac{\partial u_2^c}{\partial y}+{z_c}^3\frac{\partial u_3^c}{\partial y}\right)\right)dz_c$$

$$M_{nxx}^{C}=\int_{-\frac{h_c}{2}}^{\frac{h_c}{2}}Z_c^n\sigma_{xx}^{c}\,dz_c=\int_{-\frac{h_c}{2}}^{\frac{h_c}{2}}Z_c^n E_{xx}^{c}\,(z)\left(\left(\frac{\partial u_0^c}{\partial x}+z_c\frac{\partial u_1^c}{\partial x}+{z_c}^2\frac{\partial u_2^c}{\partial x}+{z_c}^3\frac{\partial u_3^c}{\partial x}\right)\right)\,dz_c$$

$$M_{nyy}^{C}=\int_{-\frac{h_c}{2}}^{\frac{h_c}{2}}Z_c^n\sigma_{yy}^{c}\,dz_c=\int_{-\frac{h_c}{2}}^{\frac{h_c}{2}}Z_c^n E_{yy}^{c}\,(z)\left(\left(\frac{\partial v_0^c}{\partial y}+z_c\frac{\partial v_1^c}{\partial y}+{z_c}^2\frac{\partial v_2^c}{\partial y}+{z_c}^3\frac{\partial v_3^c}{\partial y}\right)\right)dz_c \tag{23}$$

$$M_{nxy}^{C}=\int_{-\frac{h_c}{2}}^{\frac{h_c}{2}}Z_c^n\sigma_{xy}^{c}\,dz_c=\int_{-\frac{h_c}{2}}^{\frac{h_c}{2}}Z_c^n G_{xy}^{c}\,(Z)\left(\left(\frac{\partial v_0^c}{\partial x}+z_c\frac{\partial v_1^c}{\partial x}+{z_c}^2\frac{\partial v_2^c}{\partial x}+{z_c}^3\frac{\partial v_3^c}{\partial x}+\frac{\partial u_0^c}{\partial y}+z_c\frac{\partial u_1^c}{\partial y}+{z_c}^2\frac{\partial u_2^c}{\partial y}+{z_c}^3\frac{\partial u_3^c}{\partial y}\right)\right)dz_c$$

$$N_{xz}^{C}=\int_{-\frac{h_c}{2}}^{\frac{h_c}{2}}\sigma_{xz}^{c}\,dz_c=\int_{-\frac{h_c}{2}}^{\frac{h_c}{2}}G_{xz}^{c}\,(Z)\left(\frac{\partial w_0^c}{\partial x}+z_c\frac{\partial w_1^c}{\partial x}+{z_c}^2\frac{\partial w_2^c}{\partial x}+u_1^c+z_c 2u_2^c+{z_c}^2 3u_3^c\right)dZ_c$$

$$N_{yz}^{C}=\int_{-\frac{h_c}{2}}^{\frac{h_c}{2}}\sigma_{yz}^{c}\,dz_c=\int_{-\frac{h_c}{2}}^{\frac{h_c}{2}}G_{yz}^{c}\,(Z)\left(\frac{\partial w_0^c}{\partial y}+z_c\frac{\partial w_1^c}{\partial y}+{z_c}^2\frac{\partial w_2^c}{\partial y}+v_1^c+z_c 2v_2^c+{z_c}^2 3v_3^c\right)dZ_c$$

$$M_{nxz}^{C}=\int_{-\frac{h_c}{2}}^{\frac{h_c}{2}}Z_C^n\sigma_{xz}^{c}\,dz_c=\int_{-\frac{h_c}{2}}^{\frac{h_c}{2}}Z_C^n G_{xz}^{c}\,(Z)\left(\frac{\partial w_0^c}{\partial x}+z_c\frac{\partial w_1^c}{\partial x}+{z_c}^2\frac{\partial w_2^c}{\partial x}+u_1^c+z_c 2u_2^c+{z_c}^2 3u_3^c\right)dZ_c$$

$$M_{nyz}^{C}=\int_{-\frac{h_c}{2}}^{\frac{h_c}{2}}Z_C^n\sigma_{yz}^{c}\,dz_c=\int_{-\frac{h_c}{2}}^{\frac{h_c}{2}}Z_C^n G_{yz}^{c}\,(Z)\left(\frac{\partial w_0^c}{\partial y}+z_c\frac{\partial w_1^c}{\partial y}+{z_c}^2\frac{\partial w_2^c}{\partial y}+v_1^c+z_c 2v_2^c+{z_c}^2 3v_3^c\right)dZ_c$$

$$R_z^c=\int_{-\frac{h_c}{2}}^{\frac{h_c}{2}}\sigma_{zz}^{C}dZ_c=\int_{-\frac{h_c}{2}}^{\frac{h_c}{2}}E_{zz}^{C}(Z)\epsilon_{zz}^{C}dZ_c=\int_{-\frac{h_c}{2}}^{\frac{h_c}{2}}E_{zz}^{C}(z)(w_1^c+z_c 2w_2^c)dZ_c$$

$$M_z^c=\int_{-\frac{h_c}{2}}^{\frac{h_c}{2}}Z_c\,\sigma_{zz}^{C}dZ_c=\int_{-\frac{h_c}{2}}^{\frac{h_c}{2}}Z_c E_{zz}^{C}(Z)\epsilon_{zz}^{C}dZ_c=\int_{-\frac{h_c}{2}}^{\frac{h_c}{2}}Z_c E_{zz}^{C}(z)(w_1^c+2z_c w_2^c)dZ_c$$

The thick and multi-layered core layer constitutive relations connected to face sheets are stated as below given in-plane displacements by incorporating relations (13) and (12) and using relation (6). The Appendices A, B, and C contain the most important equations due to the abundance of equations.

2.8. Model of MR material:

In the period before yielding, the MR material exhibits viscoelastic behavior, elucidated through the complex modulus $G=G'+\mathrm{i}G^{"}$

where G' denotes storage modulus of the MR fluid, associated with to the average energy stored per unit volume of the material in a deformation cycle, and $G^{"}$ represents the loss modulus, which is a criterion of the energy dissipated per unit volume of the material in a cycle. The storage and loss moduli of the MR fluid were calculated for various magnetic field strengths (0, 100, 200, 300, 450, 500, and 600 G). Both moduli were represented by second-order polynomial functions relative to the field intensity[33].

$$G'(\beta) = -3.3691\beta^2 + 4.9975 \times 10^3\beta + 0.873 \times 10^6$$

$$G''(\beta) = -0.9\beta^2 + 0.8124 \times 10^3\beta + 0.1855 \times 10^6 \quad (24)$$

$$G(\beta) = G'(\beta) + iG''(\beta)$$

where β shows the magnetic field's intensityin Gauss.

no normal stress is present in the MR layer and only transverse shear stresses exist:

By placing relations (8) and (9) in the Hooke's Law expressions:

$$\sigma_{xz}^c = G(B)_{xz}^c \gamma_{xz}^c = G(B)_{xz}^c \left[\frac{\partial w_0^C}{\partial x} + z\frac{\partial w_1^C}{\partial x} + z^2\frac{\partial w_2^C}{\partial x}\right] + G(B)_{xz}^c [u_1^c + 2zu_2^c + 3z^2u_3^c] \quad (25)$$

$$\sigma_{yz}^c = G(B)_{yz}^c \gamma_{yz}^c = \sigma_{yz}^c \left[\frac{\partial w_0^C}{\partial y} + z\frac{\partial w_1^C}{\partial y} + z^2\frac{\partial w_2^C}{\partial y}\right] + G(B)_{yz}^c [v_1^c + 2zv_2^c + 3z^2v_3^c] \quad (26)$$

The anticipated reactions of the connection comply with the stipulated simply supported boundary conditions, as indicated in the subsequent relationships:

$$\begin{bmatrix} u_0^j(x,y,t) \\ v_0^j(x,y,t) \\ w_0^j(x,y,t) \\ \theta^j(x,y,t) \\ u_k^c(x,y,t) \\ v_k^c(x,y,t) \\ w_0^c(x,y,t) \end{bmatrix} = \sum_{n=1}^{\infty}\sum_{m=1}^{\infty} \begin{bmatrix} U_{0mn}^j \cos(\alpha_m x) sin(\beta_n y) \\ V_{0mn}^j \sin(\alpha_m x) cos(\beta_n y) \\ W_{0mn}^j \sin(\alpha_m x) sin(\beta_n y) \\ \theta_{0mn}^j \sin(\alpha_m x) sin(\beta_n y) \\ U_{kmn}^c \cos(\alpha_m x) sin(\beta_n y) \\ V_{kmn}^c \sin(\alpha_m x) cos(\beta_n y) \\ W_{lmn}^j \sin(\alpha_m x) sin(\beta_n y) \end{bmatrix} e^{i\omega t}, \quad (k = 0,1,2,3), (l = 0,1,2) \quad (27)$$

Where $\alpha_m = \frac{m\pi}{a}$ and $\beta_n = \frac{n\pi}{b}$

In equation (27), $W_{lmn}^j, V_{kmn}^c, U_{kmn}^c, \theta_{0mn}^j, W_{0mn}^j, U_{0mn}^j, V_{0mn}^j$ and W_{lmn}^j, denote the Fourier coefficients and "n" and "m" represent half wave numbers along "y" and "x" directions. The nonlinear ordinary differential equation is derived by inserting equations (27) into the equations of motion using displacements and imposing Galerkin's method. Solving the motion equations involves isolating each equation for the nonlinear ordinary differential by focusing on individual unknowns:

$$\{U_{0mn}^t, U_{0mn}^b, V_{0mn}^t, V_{0mn}^b, W_{0mn}^t, W_{0mn}^b, \theta_{0mn}^t, \theta_{mn}^b, U_{0mn}^c, V_{0mn}^c, u_{1mn}^c, V_{0mn}^c, W_{0mn}^c\}$$

All time-dependent variables of relations (24) are determined by the equation of motion, concerning $w(t)$, because transverse oscillations are taken into account in this article (t). The nonlinear equation of motion has the following representation in symbols:

$$\ddot{w}(t) + \omega_L^2 w(t) + \alpha_2 w(t)^2 + \alpha_3 w(t)^3 = 0 \quad (28)$$

In this relation, α_2 and α_3 coefficient of nonlinear stiffness and ω_L denotes the natural linear frequency

2.9. Solving Equation of Motion

The resulting nonlinear equation of motion (28) is tackled by perturbation methods such as the harmonic balance technique, as elucidated in [34].

2.10. Hardening/Softening Behavior in Nonlinear Oscillations

Considering [35], the following relation is used to obtain effective nonlinearity coefficient δ:

$$\delta = \frac{10a_2^2 - 9a_3\omega_L^2}{24\omega_L^2} \quad (29)$$

Thus, "δ" denotes the extent of the resonance curves bending. With δ > 0, The frequency response curves shift to right when the effective nonlinearity nature transforms into hardening. On the contrary, with δ<0, frequency-response curves curve to left as the effective nonlinearity shifts towards a softening type. Moreover, with δ = 0, the frequency-response curves show no bending either to the left or right, indicating that by the second approximation, there is a linear system response.

Based on equation (28), the quadratic nonlinearity exhibits a softening impact. When [redacted] is positive, effective nonlinearity "δ" can be either positive or negative, depending on the comparative sizes of "[redacted]" and "[redacted]".

3. FINDINGS AND DISCUSSION

3.1. Validation of the Equations

Because no study was found on the nonlinear vibrations of thick sandwich panels with MR core to date, it is necessary to compare the result of reducing the MR layer thickness —or, more accurately, the panel without the MR layer—with the current theory and the sources listed in table 2 in order to determine whether the modeling done for the thick sandwich panel was accurate.

The subsequent instances validate our research methodology.

Example: The investigation into the nonlinear free vibration of a flat rectangular panel lacking the MR layer with SSSS boundary conditions.

Here, a flat square panel devoid of a core was examined, and the outcomes of this research were contrasted with another study's findings. All mechanical specifications are taken from reference [10]. The results of these references are for a four-layer rectangular sandwich sheet and were obtained using the finite element approach. In the investigated problem, the porcelain layer is [0,90,90,0].

The data in Table 2 compares the outcomes of the present theory utilizing harmonic balance and von Karman's nonlinear strains approaches with the results derived from alternative plate theories and nonlinear strains.

Table 2. Nonlinear frequency ratio for square sandwich panel without MR layer obtained by Singh's results [4], Lal et al [10], Kumar et al.[38] and Chien's results [36] with those obtained in present model.

$A_R = w_{max}/h$ Amplitude of vibration/h	ω_{NL}/ω_L Present model	ω_{NL}/ω_L Singh's results [4]	ω_{NL}/ω_L Lal et al.[10]	ω_{NL}/ω_L Chien's results [39]	ω_{NL}/ω_L Kumar et al. results [38]	ω_{NL}/ω_L Chien's results Classical plate theory [39]
۰/۳	1.1110	۱/۰۷۹۶	۱/۰۷۳۱	۱/۰۹۸۸	1.18	1.0762
۰/۶	1.3919	۱/۲۸۶۷	۱/۲۸۵۹	۱/۳۶۲۲	1.61	1.2752
۰/۹	1.7634	۱/۵۶۹۱	۱/۵۶۵۰	۱/۷۳۷۷	2.16	1.5534

This table clearly shows that there is excellent convergence amongst the answers.

Table 3. The comparison of nonlinear frequency ratio & modal loss factor for a square sandwich panel with MR core and without MR layer .The lay-up sequences for face sheets are [0/90/0/core/0/90/0] and, β = 400, h / a = 10.

$A_R = w_{max}/h$ Amplitude of vibration/h	ω_{NL}/ω_L Present model	$\eta_{v_{NL}}/\eta_{v_L}$ Present model	ω_{NL}/ω_L Present model Without MR layer	$\eta_{v_{NL}}/\eta_{v_L}$ Present model Without MR layer
۰/۳	1.1367	0.7734	0.9940	0.9972
۰/۶	1.4727	0.4604	0.9761	0.9887
۰/۹	1.9055	0.2749	0.9455	0.9739
1.2	2.3828	0.1758	0.9015	0.9513
1.5	2.8827	0.1201	0.8423	0.9186
2	3.7412	0.0713	0.7026	0.8300

According to Table 3, it is observed that the use of magneto-rheological core reduces the vibrations of the sandwich panel by 21%.

3.2. Impact of Hardening/Softening Behavior in Nonlinear Vibrations

Table 4 indicates the mechanical properties of the face sheets concerning the MR core.

Table 4. Geometrical and mechanical characteristics of the composite sandwich panel with MR core and multi-layer face sheets [37].

Geometry	Laminate face sheets	MR Core
a=0.3m	ρ =1627 Kg/m3	ρ =3500 Kg/m^3
b=0.3m	E_1=131 GPa , E_2=E_3=10.34 GPa	$G_{12} = G_{13}$ =G_{23}= $G = G' + iG''$
h_c = 1mm	$G_{12} = G_{23}$=6.895 GPa , G_{13} = 6.205 GPa	G'= -3.3691 β^2+4.9975×10^3 β +0.873×10^6
h_t=h_b=1 mm	$v_{12} = v_{13}$ = 0.22, v_{23}=0.49	G''=-0.9 β^2+0.8124×10^3 β +0.1855×10^6

Table 5. The Values of a_3 and a_2 for flat sandwich panel with aluminum face sheet and MR core based on new sinusoidal shear deformation theory. The lay-up sequences for face sheets are [0/90/0/core/0/90/0] and β =600 G, a/b = 1, h_c/h_t = 1, m, n=1.

Magnetic Field Strengths	Effective Nonlinearity Coefficient	
β =600 G	$a_2 = -1.2256 \times 10^{-8}$	$a_3 = 1.2214 \times 10^{11}$

According to the information provided in Table 4, the impact of hardening effects surpassed that of softening effects significantly.

3.3. Discussion and numerical results about nonlinear free vibrations

This section examines the nonlinear free vibrations of a sandwich panel made of composite face sheets and an MR core as well as the impacts of varying the MR layer's thickness, aspect ratio, and magnetic field intensity on the sandwich panel's natural frequencies and modal loss factor.

3.3.1. Impact of the magnetic field intensity

The study examines the impact of magnetic field intensity loss factors and on natural frequencies of a laminated composite MR fluid sandwich plate under simply supported end conditions (SSSS) along all plate edges. The obtained results for the first modes are illustrated in Figures 3 and 4. The nonlinear frequencies show a decline as the magnetic field intensifies. Regarding the loss factor, it is calculated as the ratio between the square of the imaginary component of the complex natural frequency and the real component. Overall, there's a consistent rise in the loss factors as the magnetic field strength increases.

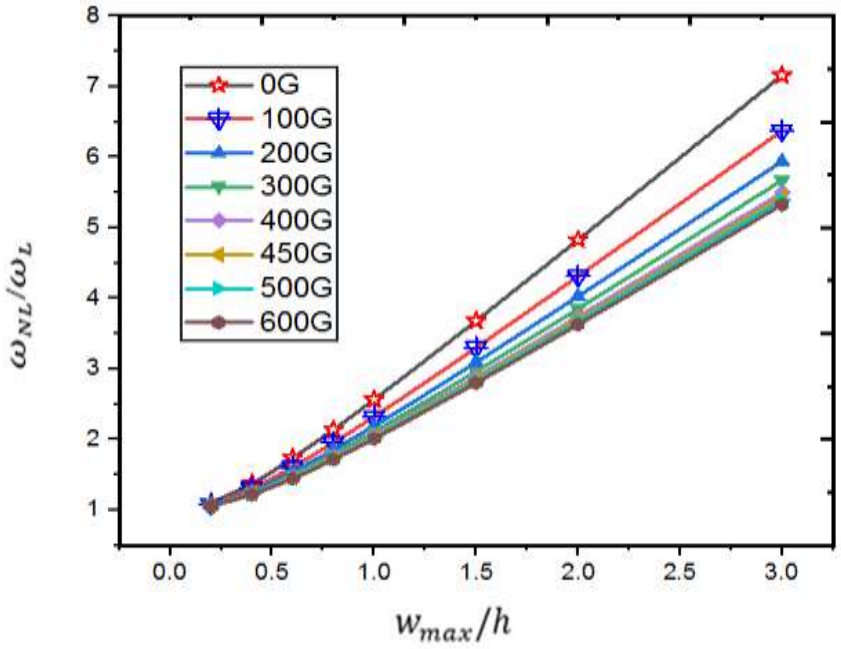

Figure 3. The graphical representations depict the nonlinear frequency ratio variations across the sheet concerning various magnetic field intensities.

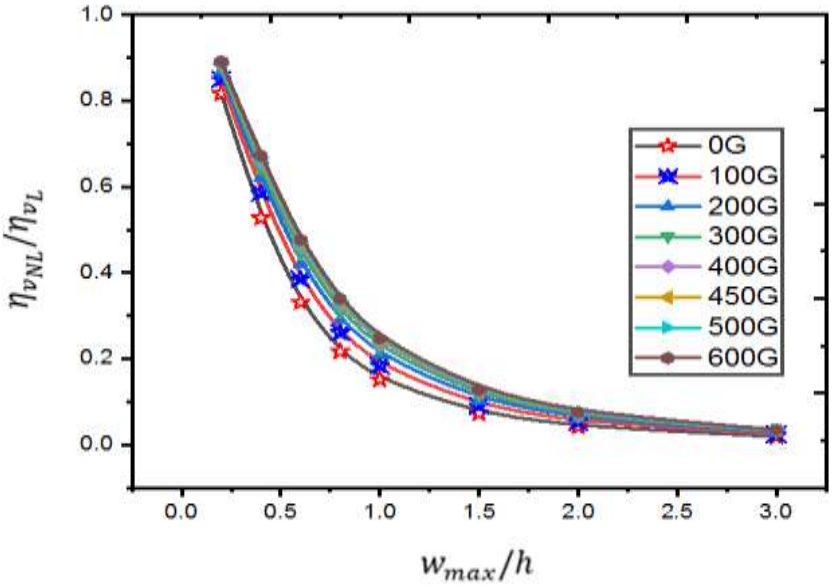

Figure 4. Diagrammatic changes damping coefficient with different Magnetic fields .

3.3.2. Impact of the MR fluid layer thickness

The study explores how changes in the thickness of the MR fluid layer affect the loss factors and nonlinear frequencies in a sandwich plate configuration ([0/90/0/ MR fluid /0/90/0]) under SSSS end conditions and a magnetic field of 450 G. Figure 5 illustrates the outcomes, showing a decrease in the nonlinear natural frequency as the MR fluid layer thickness rises. Such change may be due to a relatively greater shift in the structure's mass compared to its stiffness with increasing MR fluid layer thickness.

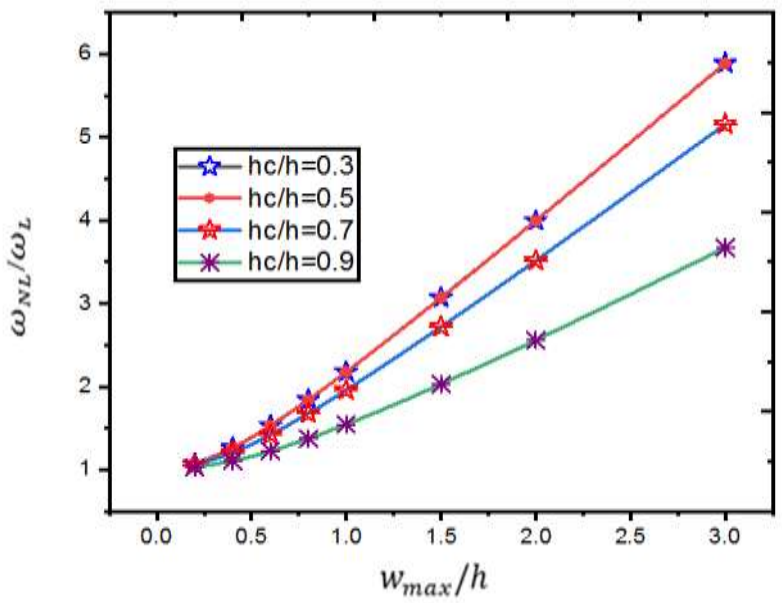

Figure 5. Diagrams of the first nonlinear changes of the sheet in varying ratios of the core to sheet thickness .

(β =450 G, a/b = 1, hc/ht = 1, m, n=1).

3.3.3. The impact of aspect ratio on the Nonlinear Frequency ratio

Figure 6 presents graphic changes in initial nonlinear frequency of a flat sandwich plate containing an MR core concerning different coefficients of aspect ratio, each associated with varying magnetic field intensities. As The plate dimensional ratio rises, indicating a thinner structure, the vibration amplitude proportionally grows. From the observations in Figure 6, it's evident that as aspect ratio increases, the sheet's natural frequency also rises. Such growth in the aspect ratio leads sheet toward a beam-like state, enhancing the transverse stiffness of the panel and consequently elevating the natural frequencies.

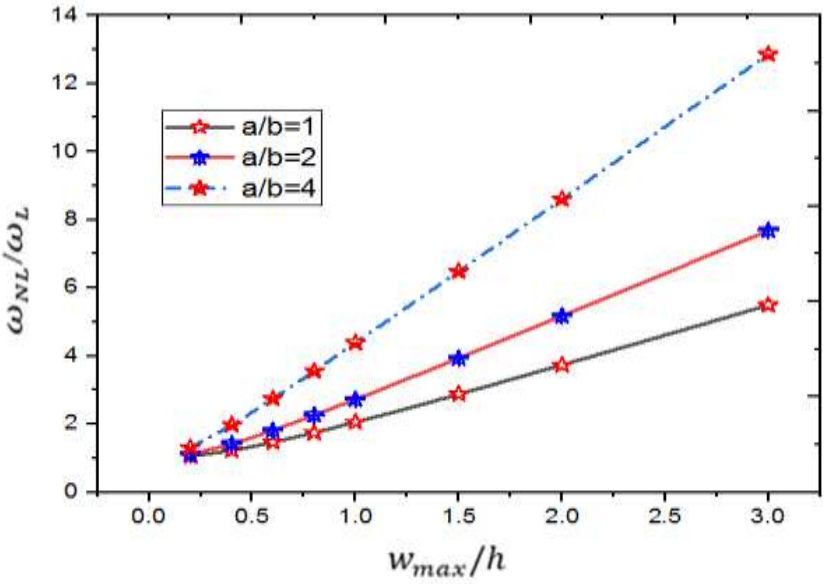

Figure 6. Diagram of the nonlinear frequency ratio variations of the sheet vs. magnetic field intensity for different aspect ratios.
(β =400 G, a/b = 1, h_c/h_t = 1, m, n=1)

3.3.4. Impact of Length-to-Thickness Ratio on the Nonlinear Frequency ratio

Figure 7,8 indicates the diagrams of the nonlinear frequency ratio and modal loss factor of the flat sandwich panel with an MR core based on the ratio of length to thickness (h_c/h_t=1, a/b =1, β =300 G).

With the increase in the sheet length to thickness ratio, the sheet's nonlinear frequency has decreased. With increasing the ratio, the sheet gets thinner, resulting in reduced stiffness. Consequently, adjusting this parameter enables obtaining the nonlinear frequency within the desired range. Moreover, the modal loss factor ratio diminishes as the vibration amplitude decreases.

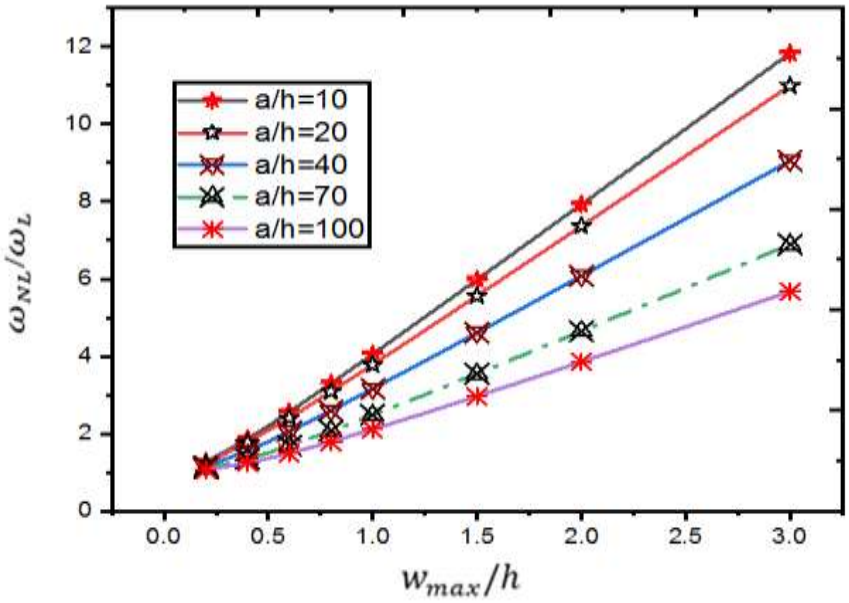

Figure 7. The variations in nonlinear frequency ratio of the sheet for varying ratios of length to thickness. *hc*/*ht*=1, a/b =1, β =300 G

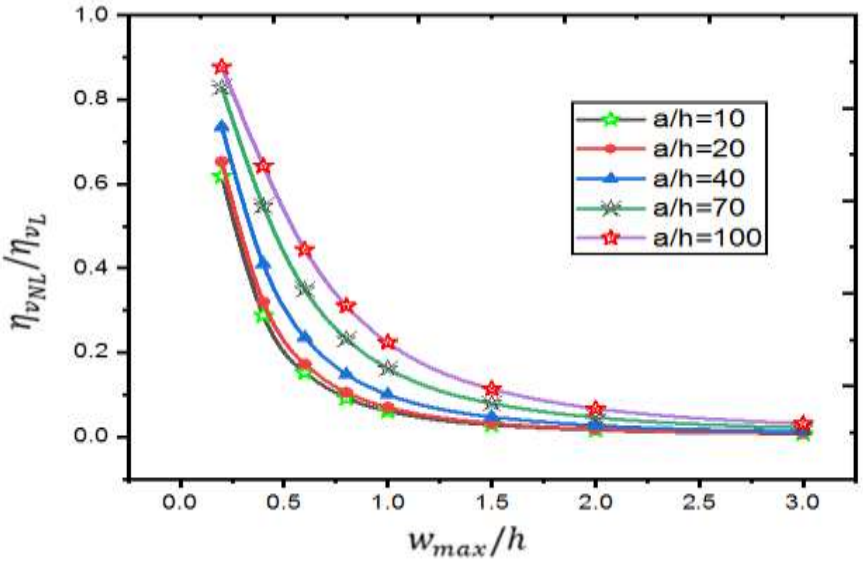

Figure 8. The modal loss factor ratio variations of the sheet for varying length to thickness ratios. *hc*/*ht*=1, a/b =1, β =300 G

HIGHLIGHTS

For controlling the nonlinear vibration behavior in sandwich panel:

• By boosting the magnetic field's intensity, the sandwich panel's nonlinear frequency is reduced.
• The panel's nonlinear frequency rises as the aspect ratio is increased.
• As the ratio of length to thickness increases, the nonlinear frequency declines.
• With the application of damping, the vibration amplitude consistently diminishes with the escalation of magnetic field intensity.
• With increasing the panel's ratio, it gets thinner, leading to a gradual increase in the vibration's amplitude.
• The nonlinear to linear frequency ratio within the MR core initially rises, then falls in line with rises in core thickness.
• The hardening behavior increases together with the thickness of the sandwich panel.

4. CONCLUSIONS

The equations governing the system and boundary conditions were derived using Hamilton's principle. We used harmonic balance technique to analytically solve the equation involving cubic and quadratic nonlinearities, and then compared the results with existing data. Galerkin's approximation was employed to transform the governing PDEs into ordinary differential equations.
The newly developed sinusoidal shear deformation plate theory offers several advantages, including simplicity, efficiency, and high accuracy in predicting the nonlinear vibration behaviors of sandwich panels featuring multi-layer face sheets and an MR fluid core. With only four unknown variables, this theory reduces computational costs and time.
The following conclusions can be formed in light of the results:

1. As the magnetic field intensity rises, the panel's nonlinear vibration frequency falls and the structure hardens, improving the stability of the structure.
2. The vibration amplitude dramatically decreases with increasing dampening and an increase in magnetic field strength.
3. The discoveries help us create a magnetic field that we can control, which allows us to alter the natural amplitude and frequency of the vibration in buildings.
4. At a consistent magnetic field intensity, the core thickness demonstrates a trend where as the panel thickness increases, the proportion of nonlinear to linear vibration frequency first elevates, followed by a gradual decrease.
5. With increasing the ratio between the core thickness and the entire panel thickness, it leads to reducing the panel stiffness.
6. Increasing the oil content in the core layer adds weight to the panel, resulting in a reduction of the panel's density-to-stiffness ratio.
7. With increasing panel's dimensional ratio, it gets thinner, leading to a gradual rise in vibration amplitude.
8. With increasing the sheet length to thickness ratio, sheet's nonlinear frequency decreased.
9. By manipulating these parameters, it's feasible to attain the preferred nonlinear vibration frequency and amplitude across various structures.

ACKNOWLEDGEMENTS

The authors express gratitude to the academic faculty and staff at the Department of Mechanical Engineering, College of Engineering, Islamic Azad University, Arak, Iran, for their support, which formed a segment of the first author's doctoral dissertation.
Funding: This study did not get dedicated financial support from public, commercial, or non-profit organizations.

Conflict of Interests: No conflict of interests with any internal or external entity in carrying out this study was declared.

Nomenclature

APPENDIX A: Descriptions of Notations

dV_t, dV_c, dV_b	The core Volume element of the top face sheet, the core and the bottom face sheet, respectively
$I_n^i (i = t, b, c)$	The moments of inertia of the top and bottom face sheets and the core
M_z^c	Normal bending moments per unit length of the edge of the core
$M_{xy}^i, M_{xx}^i, M_{yy}^i$	Bending and shear moments per unit length of the edge (i=t,b)
$M_{nxx}^c, M_{nxy}^c, M_{nyy}^c$	Shear and bending moments per unit length of the edge of the core,

M^c_{nxz}, M^c_{nyz}

$N^i_{xy}, N^i_{yx}, N^i_{xx}, N^i_{yy}$ In-plane and shear forces per unit length of the edge (i=t, b)

N^c_{xz}, N^c_{yz} Shear forces per unit length of the edge of the core

Q_{ij} The reduced stiffnesses referred to the principal material coordinates

$\bar{Q}_{ij}$ Transformed reduced stiffnesses

u_k, v_k, w_k Unknowns of the in-plane displacements of the core (k=0,1,2,3)

u_c, v_c, w_c Displacement components of the core

u^i_0, v^i_0, w^i_0 Displacement components of the face sheets, (i = t, b)

$\ddot{u}_c, \ddot{v}_c, \ddot{w}_c$ Acceleration components of the core

$\ddot{u}_i, \ddot{v}_i, \ddot{w}_i$ Acceleration components of the face sheets, (i= t, b)

Z_t, Z_b, Z_c Normal coordinates in the mid-plane of the top and the bottom face sheets and

GREEK LETTERS

ρ_t, ρ_b, ρ_c Material densities of the face sheets and the core

σ^j_{ii} Normal stress in the face sheets, (i=x,y), j=(t,b)

σ^c_{ii} Normal stress in the core, (i=x,y,z)

$\sigma^i_{xy}, \sigma^j_{xz}, \sigma^i_{yz}$ Shear stress in the face sheets, j=(t,b)

$\sigma^c_{xy}, \sigma^c_{xz}, \sigma^c_{yz}$ Shear stresses in the core

$\varepsilon^j_{0xx}, \varepsilon^j_{0xy}, \varepsilon^j_{0yy}, \varepsilon^j_{0xz}, \varepsilon^j_{0xz}$ The mid-plane strain components, (i=t,b)

$\varepsilon^c_{zz}, \varepsilon^c_{xx}, \varepsilon^c_{yy}$ Normal strains components of the core layer

$\gamma^c_{xz}, \gamma^c_{yz}, \gamma^c_{xy}$ Shear strains components of the core layer

ϕ^i_x, ϕ^i_y Rotation of the normal section of midsurface of the top face sheet and the core bottom face sheet along x and y, respectively(i=t,b)

APPENDIX B: Constitutive Equations for In-plane Stress Resultants

$$N^i_{xx} = A^i_{11}\left(\frac{\partial u^i_0}{\partial x} + \frac{1}{2}\left(\frac{\partial w^i_0}{\partial x}\right)^2\right) + B^i_{11}\frac{\partial^2 w^i_0}{\partial x^2} + D^i_{11}\frac{\partial \phi^i_x}{\partial x} + A^i_{12}\left(\frac{\partial v^i_0}{\partial y} + \frac{1}{2}\left(\frac{\partial w^i_0}{\partial y}\right)^2\right)$$
$$+B^i_{12}\frac{\partial^2 w^i_0}{\partial y^2} + D^i_{12}\frac{\partial \phi^i_y}{\partial y} + A^i_{16}\left(\frac{\partial u^i_0}{\partial y} + \frac{\partial v^i_0}{\partial x} + \frac{\partial w^i_0}{\partial x}\frac{\partial w^i_0}{\partial y}\right) + B^i_{16}\left(2\,\frac{\partial^2 W^i_0}{\partial x \partial y}\right) + D^i_{16}\left(\frac{\partial \phi^i_x}{\partial y} + \frac{\partial \phi^i_y}{\partial x}\right)$$

$$P^i_{xx} = E^i_{11}\left(\frac{\partial u^i_0}{\partial x} + \frac{1}{2}\left(\frac{\partial w^i_0}{\partial x}\right)^2\right) + G^i_{11}\frac{\partial^2 w^i_0}{\partial x^2} + H^i_{11}\frac{\partial \phi^i_x}{\partial x} + E^i_{12}\left(\frac{\partial v^i_0}{\partial y} + \frac{1}{2}\left(\frac{\partial w^i_0}{\partial y}\right)^2\right)$$
$$+G^i_{12}\frac{\partial^2 w^i_0}{\partial y^2} + H^i_{12}\frac{\partial \phi^i_y}{\partial y} + E^i_{16}\left(\frac{\partial u^i_0}{\partial y} + \frac{\partial v^i_0}{\partial x} + \frac{\partial w^i_0}{\partial x}\frac{\partial w^i_0}{\partial y}\right) + G^i_{16}\left(2\,\frac{\partial^2 W^i_0}{\partial x \partial y}\right) + H^i_{16}\left(\frac{\partial \phi^i_x}{\partial y} + \frac{\partial \phi^i_y}{\partial x}\right)$$

$$S^i_{yz} = K_S\left[J^i_{44}\left(\frac{\partial w^i_0}{\partial y}\right) + G^i_{44}\frac{\partial w^i_0}{\partial y} + H^i_{44}\phi^i_y + A^i_{45}\left(\frac{\partial w^i_0}{\partial x}\right) + G^i_{45}\frac{\partial w^i_0}{\partial x} + H^i_{45}\phi^i_x\right]$$

In the above equations, the stiffness coefficients for multilayer sheets are defined as follows:

$$\int_{-\frac{h_i}{2}}^{\frac{h_i}{2}} \bar{Q}_{11} dZ_i = A^i_{11} \qquad \int_{-\frac{h_i}{2}}^{\frac{h_i}{2}} \bar{Q}_{11} f_1(z_i)\, dZ_i = B^i_{11} \qquad \int_{-\frac{h_i}{2}}^{\frac{h_i}{2}} \bar{Q}_{11}\, f_2(z_i)\, dZ_i = D^i_{11}$$

$$\int_{-\frac{h_i}{2}}^{\frac{h_i}{2}} \bar{Q}_{11}\, f_1(z_i)\, dZ_i = B^i_{11}\ , \int_{-\frac{h_i}{2}}^{\frac{h_i}{2}} \bar{Q}_{11} f_1(z_i) f_1(z_i)\, dZ_i = F^i_{11}\ , \int_{-\frac{h_i}{2}}^{\frac{h_i}{2}} \bar{Q}_{11}\, f_2(z_i) f_1(z_i)\, dZ_i = G^i_{11}$$

$$\int_{-\frac{h_i}{2}}^{\frac{h_i}{2}} \bar{Q}_{12} f_2(z_i) dZ_i = E^i_{12}\ , \int_{-\frac{h_i}{2}}^{\frac{h_i}{2}} \bar{Q}_{12} f_2(z_i)\, f_1(z_i) dZ_i = G^i_{12}\ , \int_{-\frac{h_i}{2}}^{\frac{h_i}{2}} \bar{Q}_{12}\, f_2(z_i)\, f_2(z_i) dZ_i = H^i_{12}$$

APPENDIX C: Constitutive Equations for thick core layer

To define the motion equations in terms of displacement, and to facilitate solving the motion equations, the following integrals are applied:

$$e^{c(xx)}_n = \int_{-\frac{h_c}{2}}^{\frac{h_c}{2}} Z_c E^C_{xx}(Z)\, dz\ ,\ e^{c(yy)}_n = \int_{-\frac{h_c}{2}}^{\frac{h_c}{2}} Z_c E^C_{yy}(Z)\, dz\ ,\ \mathrm{g}^{c(xy)}_n = \int_{-\frac{h_c}{2}}^{\frac{h_c}{2}} Z^n_c G^C_{xy}(Z)\, dz \qquad n = 0,1,2,3$$

$$\mathrm{g}^{c(xz)}_n = \int_{-\frac{h_c}{2}}^{\frac{h_c}{2}} Z^n_c G^C_{(xz)}(Z)\, dz\ ,\ \ \mathrm{g}^{c(yz)}_n = \int_{-\frac{h_c}{2}}^{\frac{h_c}{2}} Z^n_c G^C_{(yz)}(Z)\, dz \qquad n = 0,1,2$$

By applying the above equations to the fundamental tension equations of the core, they can be written as follows:

$$N_{xx}^{c} = e_0^{c(xx)} \frac{\partial u_0^c}{\partial x} + e_1^{c(xx)} \frac{\partial u_1^c}{\partial x} + e_2^{c(xx)} \frac{\partial u_2^c}{\partial x} + e_3^{c(xx)} \frac{\partial u_3^c}{\partial x}$$

$$M_{nxx}^{c} = e_n^{c(xx)} \frac{\partial u_0^c}{\partial x} + e_{n+1}^{c(xx)} \frac{\partial u_1^c}{\partial x} + e_{n+2}^{c(xx)} \frac{\partial u_2^c}{\partial x} + e_{n+3}^{c(xx)} \frac{\partial u_3^c}{\partial x}$$

$$R_z^c = \mathrm{e}_0^{c(xz)} w_1^c + 2\mathrm{e}_1^{c(xz)} w_2^c$$

$$M_z^c = \mathrm{e}_1^{c(xz)} w_1^c + 2\mathrm{g}_2^{c(xz)} w_2^c$$

5.REFERENCES

1. Chandra, R., Large deflection vibration of cross-ply laminated plates with certain edge conditions. Journal of Sound and Vibration, 1976. 47(4): p. 509-514.
2. Chandra, R. and B.B. Raju, Large deflection vibration of angle ply laminated plates. Journal of Sound and Vibration, 1975. 40(3): p. 393-408.
3. Singh, G., et al., Non-linear vibrations of simply supported rectangular cross-ply plates. Journal of Sound and Vibration, 1990. 142(2): p. 213-226.
4. Singh, G., G.V. Rao, and N. Lyengar, Large amplitude free vibration of simply supported antisymmetric cross-ply plates. AIAA journal, 1991. 29(5): p. 784-790.
5. Amabili, M., K. Karazis, and K. Khorshidi, Nonlinear vibrations of rectangular laminated composite plates with different boundary conditions. International Journal of Structural Stability and Dynamics, 2011. 11(04): p. 673-695.
6. Khorshidi, K., Analytical nonlinear elasto-plastic impact response of a moderately thick rectangular plate. 2010.
7. Yazdi, A.A., Homotopy perturbation method for nonlinear vibration analysis of functionally graded plate. Journal of Vibration and Acoustics, 2013. 135(2): p. 021012.
8. Quan, T.Q., et al., Vibration and nonlinear dynamic response of imperfect sandwich piezoelectric auxetic plate. Mechanics of Advanced Materials and Structures, 2022. 29(1): p. 127-137.
9. Li, J.-J. and C.-J. Cheng, Differential quadrature method for nonlinear vibration of orthotropic plates with finite deformation and transverse shear effect. Journal of Sound and Vibration, 2005. 281(1-2): p. 295-309.
10. Lal, A., B. Singh, and R. Kumar, Nonlinear free vibration of laminated composite plates on elastic foundation with random system properties. International Journal of Mechanical Sciences, 2008. 50(7): p. 1203-1212.
11. Tian, A., R. Ye, and Y. Chen, A new higher order analysis model for sandwich plates with flexible core. Journal of Composite Materials, 2016. 50(7): p. 949-961.
12. Malekzadeh, K., et al., Dynamic response of in-plane pre-stressed sandwich panels with a viscoelastic flexible core and different boundary conditions. Journal of composite materials, 2006. 40(16): p. 1449-1469.
13. Frostig, Y. and O.T. Thomsen, High-order free vibration of sandwich panels with a flexible core. International Journal of Solids and Structures, 2004. 41(5-6): p. 1697-1724.
14. Malekzadeh, K., M. Khalili, and R. Mittal, Local and global damped vibrations of plates with a viscoelastic soft flexible core: an improved high-order approach. Journal of Sandwich Structures & Materials, 2005. 7(5): p. 431-456.
15. Eshaghi, M., R. Sedaghati, and S. Rakheja, Dynamic characteristics and control of magnetorheological/electrorheological sandwich structures: a state-of-the-art review. Journal of Intelligent Material Systems and Structures, 2016. 27(15): p. 2003-2037.
16. Carlson, J.D., What makes a good MR fluid? Journal of intelligent material systems and structures, 2002. 13(7-8): p. 431-435.
17. Yeh, J.-Y. and L.-W. Chen, Vibration of a sandwich plate with a constrained layer and electrorheological fluid core. Composite structures, 2004. 65(2): p. 251-258.
18. Yeh, J.-Y. and L.-W. Chen, Finite element dynamic analysis of orthotropic sandwich plates with an electrorheological fluid core layer. Composite structures, 2007. 78(3): p. 368-376.
19. Yeh, J.-Y. and L.-W. Chen, Dynamic stability analysis of a rectangular orthotropic sandwich plate with an electrorheological fluid core. Composite structures, 2006. 72(1): p. 33-41.
20. Yeh, J.-Y., Vibration analyses of the annular plate with electrorheological fluid damping treatment. Finite Elements in Analysis and Design, 2007. 43(11-12): p. 965-974.
21. Yeh, J.-Y., et al., Damping and vibration analysis of polar orthotropic annular plates with ER treatment. Journal of Sound and Vibration, 2009. 325(1-2): p. 1-13.
22. Yeh, J.-Y., Free vibration analysis of rotating polar orthotropic annular plate with ER damping treatment. Composites Part B: Engineering, 2011. 42(4): p. 781-788.
23. Keshavarzian, M., et al., High-order analysis of linear vibrations of a moderatleythick sandwich panel with an electrorheological core. Mechanics of Advanced Composite Structures, 2020. 7(2): p. 177-188.
24. Keshavarzian, M., et al., Non-linear free vibration analysis of a thick sandwich panel with an electrorheological core. Journal of Vibration Engineering & Technologies, 2022. 10(4): p. 1495-1509.

25. Keshavarzian, M., et al., Comparison of the application of smart electrorheological and magnetorheological fluid cores to damp sandwich panels' vibration behavior, based on a novel higher-order shear deformation theory. Proceedings of the Institution of Mechanical Engineers, Part E: Journal of Process Mechanical Engineering, 2022. 236(2): p. 225-244.
26. Nayak, B., S. Dwivedy, and K. Murthy, Dynamic analysis of magnetorheological elastomer-based sandwich beam with conductive skins under various boundary conditions. Journal of Sound and Vibration, 2011. 330(9): p. 1837-1859.
27. Li, Y.-H., et al., Dynamic analysis of sandwich plates with a constraining layer and a magnetorheological fluid core. Polymers and Polymer Composites, 2011. 19(4-5): p. 295-302.
28. Reddy, J.N., Mechanics of laminated composite plates and shells: theory and analysis. 2003: CRC press.
29. Sayyad, A.S. and Y.M. Ghugal, Bending and free vibration analysis of thick isotropic plates by using exponential shear deformation theory. Applied and Computational mechanics, 2012. 6(1).
30. Wang, Q., A. Yao, and M.H. Dindarloo, New higher-order shear deformation theory for bending analysis of the two-dimensionally functionally graded nanoplates. Proceedings of the Institution of Mechanical Engineers, Part C: Journal of Mechanical Engineering Science, 2021. 235(16): p. 3015-3028.
31. Phuc, P.M. and V.N. Thanh, A new sinusoidal shear deformation theory for static bending analysis of functionally graded plates resting on Winkler–Pasternak foundations. Advances in Civil Engineering, 2021. 2021(1): p. 6645211.
33. Fard, K.M., M. Livani, and F.A. Ghasemi, Improved high order free vibration analysis of thick double curved sandwich panels with transversely flexible cores. Latin American Journal of Solids and Structures, 2014. 11: p. 2284-2307.
33. Rajamohan, V., R. Sedaghati, and S. Rakheja, Vibration analysis of a multi-layer beam containing magnetorheological fluid. Smart Materials and Structures, 2009. 19(1): p. 015013.
34. Nayfeh, A., J. Nayfeh, and D. Mook, On methods for continuous systems with quadratic and cubic nonlinearities. Nonlinear Dynamics, 1992. 3: p. 145-162.
35. Onkar, A.K. and D. Yadav, Non-linear free vibration of laminated composite plate with random material properties. Journal of Sound and Vibration, 2004. 272(3-5): p. 627-641.
36. Chien, R.-D. and C.-S. Chen, Nonlinear vibration of laminated plates on an elastic foundation. Thin-walled structures, 2006. 44(8): p. 852-860.
37. Manoharan, R., R. Vasudevan, and A. Jeevanantham, Dynamic characterization of a laminated composite magnetorheological fluid sandwich plate. Smart Materials and Structures, 2014. 23(2): p. 025022.